ORIGINAL ARTICLE

Evacetrapib: in vitro and clinical disposition, metabolism, excretion, and assessment of drug interaction potential with strong CYP3A and CYP2C8 inhibitors

Ellen A. Cannady, Ming-Dauh Wang, Stuart Friedrich, Jessica L. F. Rehmel, Ping Yi, David S. Small, Wei Zhang & Jeffrey G. Suico[a]

Departments of Clinical Pharmacology, Drug Disposition, Medical, and Statistics, Lilly Research Laboratories, Eli Lilly and Company, Indianapolis, Indiana

Abstract

Evacetrapib is an investigational cholesteryl ester transfer protein inhibitor (CETPi) for reduction of risk of major adverse cardiovascular events in patients with high-risk vascular disease. Understanding evacetrapib disposition, metabolism, and the potential for drug–drug interactions (DDI) may help guide prescribing recommendations. In vitro, evacetrapib metabolism was investigated with a panel of human recombinant cytochromes P450 (CYP). The disposition, metabolism, and excretion of evacetrapib following a single 100-mg oral dose of ^{14}C-evacetrapib were determined in healthy subjects, and the pharmacokinetics of evacetrapib were evaluated in the presence of strong CYP3A or CYP2C8 inhibitors. In vitro, CYP3A was responsible for about 90% of evacetrapib's CYP-associated clearance, while CYP2C8 accounted for about 10%. In the clinical disposition study, only evacetrapib and two minor metabolites circulated in plasma. Evacetrapib metabolism was extensive. A mean of 93.1% and 2.30% of the dose was excreted in feces and urine, respectively. In clinical DDI studies, the ratios of geometric least squares means for evacetrapib with/without the CYP3A inhibitor ketoconazole were 2.37 for area under the curve $(AUC)_{(0-\infty)}$ and 1.94 for C_{max}. There was no significant difference in evacetrapib $AUC_{(0-\tau)}$ or C_{max} with/without the CYP2C8 inhibitor gemfibrozil, with ratios of 0.996 and 1.02, respectively. Although in vitro results indicated that both CYP3A and CYP2C8 metabolized evacetrapib, clinical studies confirmed that evacetrapib is primarily metabolized by CYP3A. However, given the modest increase in evacetrapib exposure and robust clinical safety profile to date, there is a low likelihood of clinically relevant DDI with concomitant use of strong CYP3A or CYP2C8 inhibitors.

Abbreviations

AUC, area under the curve; BMI, body mass index; CETPi, cholesteryl ester transfer protein inhibitor; CPM, counts per minute; DDI, drug–drug interaction; HDL-C, high-density lipoprotein cholesterol; LDL-C, low-density lipoprotein cholesterol; LSC, liquid scintillation counting; NMR, nuclear magnetic resonance; PD, pharmacodynamic; P-gp, P-glycoprotein; PK, pharmacokinetics; RAF, relative activity factor; TEAEs, treatment-emergent adverse events.

Introduction

Aggressive lowering of low-density lipoprotein cholesterol (LDL-C), mainly through the use of lipid-lowering therapies such as HMG-CoA reductase inhibitors (statins), has demonstrated 20–35% relative reductions in cardiovascular events (Heart Protection Study Collaborative Group 2002; Shepherd et al. 2002; Sever et al. 2003; Cannon et al. 2004). Despite progress in reducing cardiovascular disease risk, there remains a need for therapies targeting other risk factors such as lower than recommended levels of high-density lipoprotein cholesterol (HDL-C). Inhibition of the cholesteryl ester transfer protein (CETP), leads to a substantial increase in HDL-C levels (Barter et al. 2003). Such an approach may reduce residual cardiovascular risk, given the hypothesized inverse relationship between cardiovascular risk and HDL-C levels (Brown et al. 2001; Robins et al. 2001; deGoma et al. 2008).

Evacetrapib, a potent and selective inhibitor of CETP, is being evaluated for its potential to reduce the risk of major adverse cardiovascular events in patients with high-risk vascular disease. To date, evacetrapib has been well tolerated in clinical studies and has demonstrated a clinically relevant pharmacodynamic (PD) effect in early-phase development (Nicholls et al. 2011; Suico et al. 2014). Evacetrapib has not demonstrated the off-target liabilities associated with torcetrapib, a CETP inhibitor that was terminated in late-phase development (Joy and Hegele 2008). In patients with dyslipidemia, evacetrapib given alone or with statins increased HDL-C levels and decreased LDL-C levels without producing substantial changes in blood pressure, aldosterone, cortisol, or electrolytes (Nicholls et al. 2011).

The patient population taking evacetrapib will likely be on multiple concomitant medications. To fully understand the benefit : risk profile of evacetrapib, it is important to understand the drug–drug interaction (DDI) potential of medications that might affect the pharmacokinetics (PK) of evacetrapib, as well as the effects of evacetrapib on the PK of other drugs. The latter will be described in a separate manuscript. This article presents data from in vitro, clinical disposition/metabolism/excretion, and DDI studies evaluating the effects of strong CYP3A and CYP2C8 inhibitors on the PK of evacetrapib. Although the in vitro results showed that CYP3A is predominately responsible for the oxidative clearance of evacetrapib, clinical studies conducted with a concomitantly administered potent CYP3A inhibitor resulted in a modest change in the PK profile of evacetrapib, while a strong CYP2C8 inhibitor had minimal effect on evacetrapib exposure.

Material and Methods

Identifying human CYP450s capable of metabolizing evacetrapib, and predicting contributions to hepatic CYP-mediated clearance

Evacetrapib was synthesized at Eli Lilly and Company. Human liver microsomes (HLMs) from a mixed sex pool of 10 individuals were purchased from XenoTech, LLC (Lenexa, KS). A panel of human recombinant CYPs (rCYPs), provided as Supersomes™ (microsomes prepared from insect cells engineered to over-express cDNA for human CYPs, were co-expressed with CYPb$_5$, if available) as well as membrane control (no CYP). Supersomes™ were obtained from BD Gentest (Woburn, MA). The panel of 10 human rCYPs evaluated is commonly involved in human drug metabolism and include rCYPs 1A2, 2B6, 2C8, 2C9, 2C19, 2D6, 2E1, 2J2, 3A4, and 3A5.

Incubations and calculations were performed as presented in Wickremsinhe et al. (2014). Briefly, incubations containing positive control (verapamil) or evacetrapib (30 or 300 nmol/L), matrix (HLMs, rCYPs as Supersomes™, or membrane control; 0.25 mg/mL), and buffer were initiated with NADPH (1 mmol/L) and reactions were stopped after 5 or 30 mins with acetonitrile and internal standard. Signals identified and verified through a multifactorial approach were considered quantifiable. Intrinsic clearance (CL$_{int}$) in rCYPs was scaled to HLM-scaled CL$_{int}$ as:

$$\text{HLM-scaled CL}_{int} = -k_{dep} \times (\text{Incubation volume/pmol rCYP}) \times \text{RAF},$$

where $-k_{dep}$ is the negative of the substrate depletion rate constant (min^{-1}), pmol rCYP is the lot-specific amount of rCYP in the incubation, and relative activity factor (RAF) is a relative activity factor (pmol/mg) appropriate for the rCYPs/HLMs pair. The fraction of hepatic CYP-mediated clearance (f$_m$CYP) for each rCYP yielding a quantifiable signal was determined by dividing the HLM-scaled CL$_{int}$ by the sum of all quantified HLM-scaled CL$_{int}$.

After calculating f$_m$CYP, a static model was applied to estimate the effect of complete inhibition of each participating CYP on the area under the curve (AUC) of evacetrapib concentration versus time after oral dosing. The model was modified from Fahmi et al. 2008 and assumes that intestinal metabolism is negligible. The fraction eliminated by CYPs was estimated from the phase I [^{14}C] study described herein.

$$AUCi/AUC = 1/(1-f_mCYP \times \text{fraction of evacetrapib eliminated by CYPs})$$

Clinical studies

Three clinical studies contributing data to this manuscript were conducted in accordance with the Declaration of Helsinki and the International Conference on Harmonisation Good Clinical Practice guidelines and with the approval of the local ethics committee. For the evacetrapib disposition study, the Clinical Research Unit was located in Madison, WI, and the study protocol was reviewed by Independent Investigational Review Board (Plantation, FL). The evacetrapib ± ketoconazole trial was reviewed by Independent Investigational Review Board and conducted at 2 sites. The evacetrapib ± gemfibrozil study was conducted in Daytona Beach, FL, and reviewed by Schulman Associated IRB (Ft. Lauderdale, FL). All ethics committees maintain full accreditation with the Association for the Accreditation of Human Research Protection Programs. Each subject gave their informed written consent.

Study population

The studies enrolled healthy subjects aged 18–65 years old with body mass index (BMI) of 18–32 kg/m^2. Subjects enrolled in the studies were not allowed to eat the fruit or drink the juice from grapefruit or Seville oranges for 7 days prior to the start of the study, were not to be taking prescription, over-the counter, or herbal medications within 14 days of admission to the study, were to have limited alcohol consumption, and were to be considered nonsmokers, which included use of tobacco or nicotine replacement products.

Phase 1 disposition, metabolism and excretion study with evacetrapib in healthy subjects

An open-label phase 1 study assessed the disposition of radioactivity and evacetrapib in five healthy males after a single, oral 100-mg dose of evacetrapib containing approximately 100 μCi [^{14}C]-evacetrapib. Following oral administration of [^{14}C]-evacetrapib, sequential postdose blood samples were collected out to 192 h to determine evacetrapib concentrations for use in calculating PK parameter estimates of evacetrapib and to identify excreted metabolites. Sequential urine and fecal samples up to 216 h postdose were collected to determine the mass balance of [^{14}C]-evacetrapib and to identify metabolites in these matrices. Samples of expired air were also collected at selected time points up to 48 h for the analysis of $^{14}CO_2$. Subjects were discharged when at least 90%

of the administered radioactivity had been recovered or 24-h urine and fecal samples from 2 consecutive 24-h collections each had radioactivity levels less than 1.0% of the total administered radioactivity in urine and feces combined.

Phase 1 DDI study with ketoconazole in healthy subjects

This study used a randomized, open-label, 2-period, fixed-sequence design to evaluate the effect of ketoconazole on the PK of evacetrapib (Fig. S1). Fasted healthy adult males and females ($N = 12$, 18–65 years), with a BMI of 18–32 kg/m^2, received a single 100-mg oral dose of evacetrapib in Period 1, after which there was a minimum 14-day washout based on the evacetrapib mean half-life of approximately 40 h. In Period 2, 12 healthy subjects received 14 daily oral doses of 400-mg ketoconazole, which is an adequate ketoconazole dose to inhibit CYP3A (Zhao et al. 2009; Han et al. 2013), with a concomitantly administered single 100-mg dose of evacetrapib administered on Day 5. Blood samples were collected in both periods to determine plasma concentrations of evacetrapib. In Period 1, blood samples were collected from predose through 168 h postdose. In Period 2, evacetrapib blood samples were collected starting on Day 5 (predose) and continuing for 240 h after the dose of evacetrapib was administered.

Phase 1 DDI study with gemfibrozil in healthy subjects

This was a phase 1, fixed-sequence, 3-period study to assess the effect of gemfibrozil on the PK of evacetrapib in healthy adults (Fig. S2). A secondary objective of the study was to evaluate the effects of evacetrapib on the PK of gemfibrozil. Eligible subjects ($N = 24$) were healthy adult males or females 18–65 years old with a BMI of 18–32 kg/m^2.

In Period 1, subjects received a single oral dose of 600 mg gemfibrozil in the morning on Day 1. In Period 2, subjects received daily oral doses of 130 mg evacetrapib for 11 days (Days 2–12). In Period 3, subjects received twice-daily oral doses of 600 mg gemfibrozil in addition to once-daily doses of 130 mg evacetrapib for 10 days (Days 13 to 22), with a final morning dose of 600 mg gemfibrozil on Day 23. Evacetrapib was administered approximately 1 h after gemfibrozil administration. The dose and dose frequency of gemfibrozil administration used in this study was deemed appropriate, as in silico predictions have suggested that treatment with 600 mg gemfibrozil twice daily (BID) for at least 5 days would be sufficient to inhibit >98% of CYP2C8 activity via the mechanism based inactivation of the enzyme by the 1-O-β-glucuronide metabolite

of gemfibrozil (Honkalammi et al. 2012). Blood samples were collected to determine the plasma concentrations of both evacetrapib and gemfibrozil. In Period 1, blood samples were collected to determine plasma concentrations of gemfibrozil through 12 h postdose (Day 1). In Period 2, blood samples were collected through 24-h postdose following the tenth daily dose of evacetrapib (Day 11). In Period 3, blood samples were collected to determine evacetrapib plasma concentrations through 24-h postdose following the last dose of evacetrapib administered on Day 22. Blood samples were collected to determine gemfibrozil plasma concentrations through 12-h postdose following the first dose of gemfibrozil, which was administered on the morning of Day 13.

Bioanalysis and radioanalysis

Plasma samples were analyzed for evacetrapib using a validated LC/MS/MS method (data on file; BASi [West Lafayette, IN] for the evacetrapib disposition study and Covance Laboratories, Inc. [Madison, WI] for the evacetrapib ± ketoconazole and evacetrapib ± gemfibrozil studies). For all three studies, the dynamic range for the evacetrapib assay was 1–1000 ng/mL. Samples above the upper limit of quantification were diluted and reanalyzed to yield results within the calibrated range. For the evacetrapib disposition, evacetrapib ± ketoconazole, and evacetrapib ± gemfibrozil studies, during validation, the inter-assay accuracy (relative error) ranged from −6.0% to 6.2%, −1.4% to 4.3%, and −0.7% to 1.5%, respectively; the inter-assay precision (relative standard deviation) ranged from 2.1% to 6.4%, 3.7% to 8.6%, and 2.9% to 4.8%, respectively.

Plasma samples were analyzed for gemfibrozil and gemfibrozil 1-O-β-glucuronide using a validated LC/MS/MS method (data on file; Advion Bioanalytical Labs, A Quintiles Company [Ithaca, NY]). The dynamic range of the assay for both analytes was 5–10,000 ng/mL. The inter-assay accuracy ranged from −10.6% to 5.81% and −11.6% to 1.85% for gemfibrozil and the metabolite, respectively. The inter-assay precision ranged from 3.35% to 4.92% and 2.95% to 9.05% for gemfibrozil and the metabolite, respectively.

In the evacetrapib disposition study, radioactivity in all samples was measured by liquid scintillation counting (LSC). Radioactivity in whole blood, plasma, expired air, urine, and feces was determined using LSC techniques either directly (in urine, plasma, and expired air) or after combustion in an oxidizer apparatus (in feces and blood). The cumulative fraction of the dose eliminated in excreta was determined by measuring the amount of radioactivity in the urine and feces for each collection period, up to 216 h postdose. The radioactivity analyses were conducted at Covance Laboratories, Inc.

Pharmacokinetic analyses

In all three studies, PK parameter estimates for evacetrapib were calculated by standard noncompartmental methods of analysis (Version 5.2; WinNonlin, Pharsight Corporation, Mountain View, CA, USA). The primary parameters were maximum concentration (C_{max}) and AUC of evacetrapib.

Metabolite radioprofiling and identification by LC/MS

Plasma, fecal, and urine samples were extracted, dried and reconstituted in a mixture containing dimethylsulfoxide, acetonitrile, and 10 mmol/L ammonium acetate (1:3:3, v:v:v) for radioprofiling and metabolite identification [Eli Lilly and Company; Indianapolis, IN]. For radioprofiling, metabolites in various matrices were separated by HPLC and collected into 96-well scintiplates for radioactivity counting and radiochromatogram reconstruction. For metabolite identification, LC/MS and LC/MS/MS data were generated on a Finnigan LCQ Advantage ion trap mass spectrometer for nominal mass measurement and on a Finnigan LTQ Orbitrap XL mass spectrometer for accurate mass measurement (Thermo Electron, San Jose, CA) in positive ion mode.

Metabolite identification by nuclear magnetic resonance

Major fecal metabolites M1 and M7 were isolated using reverse-phase semi-preparative HPLC system and analyzed (Eli Lilly and Company) using a Bruker AVANCE 600 nuclear magnetic resonance (NMR) (Bruker BioSpin Corporation, Billerica, MA).

Statistical analysis

In the evacetrapib ± ketoconazole and evacetrapib ± gemfibrozil studies, evacetrapib AUC and C_{max} were log-transformed and analyzed using an ANOVA model, using treatment as a fixed effect and subject as a random effect, to provide estimates of geometric means, ratios of the geometric means (evacetrapib + ketoconazole or evacetrapib + gemfibrozil vs. evacetrapib alone), and their 90% confidence intervals (CIs). The t_{max} for evacetrapib was analyzed using a Wilcoxon sign rank test.

Safety assessments

In all three studies, safety measurements included recording adverse events and evaluation of clinical laboratory data.

Results

Identifying human CYP450s capable of metabolising evacetrapib with prediction of contributions to hepatic CYP-mediated clearance and application of a static DDI model

The positive control, verapamil, demonstrated the expected substrate depletion rate constant, k, in HLMs and metabolism by rCYP2D6, rCYP3A4, and rCYP3A5 (Eli Lilly and Company, unpubl. data). Evacetrapib depletion in HLMs was observed, but did not meet the criteria for first order depletion; thus, the largest k calculated for evacetrapib in HLMs (0.0345 min^{-1}) was used to approximate first-order conditions. The resulting CL$_{int}$ for evacetrapib in HLMs was 138 μL $\times$ min^{-1} $\times$ mg^{-1}. For evacetrapib, depletion by rCYP2C8, rCYP3A4, and rCYP3A5 met the criteria for quantification. For determinations of f_m, CYP3A4-mediated metabolism was considered to represent total CYP3A-mediated metabolism. rCYP CL$_{int}$ values of 0.712 μL $\times$ min^{-1} $\times$ pmol^{-1} for rCYP2C8 and 4.257 μL $\times$ min^{-1} $\times$ pmol^{-1} for rCYP3A were estimated for evacetrapib (Table 1). Using predetermined RAFs, HLM-scaled CLint for CYP2C8 was estimated to be 19.9 μL $\times$ min^{-1} $\times$ mg^{-1}. HLM-scaled CL$_{int}$ for CYP3A was estimated to be 186 μL $\times$ min^{-1} $\times$ mg^{-1}. The resulting f_mCYP values for the hepatic CYP-mediated clearance of evacetrapib were 0.1 for CYP2C8 and 0.9 for CYP3A, suggesting that CYP2C8 is responsible for 10% and CYP3A is responsible for 90% of the hepatic CYP-mediated clearance of evacetrapib. This estimate does not include any potential non-CYP hepatic metabolic pathways (e.g., glucuronidation). The resulting static model predicted the clinical AUC$_i$/AUC ratios for inhibition of CYP2C8 and CYP3A to be 1.1 and 2.7, respectively.

Phase 1 disposition and pharmacokinetic study in healthy subjects

Pharmacokinetics of evacetrapib and radioactivity in plasma and blood

Pharmacokinetic parameter estimates for evacetrapib in plasma and for total radioactivity in plasma and blood are presented in Table 2. Following C_{max}, plasma concentrations of evacetrapib declined in a multiphasic manner. The C_{max} of total radioactivity was greater than the C_{max} of evacetrapib, which indicates the presence of circulating radioactive entities other than evacetrapib. Blood-to-plasma total radioactivity ratios combined with the hematocrit values suggest negligible association of

evacetrapib-related material with red blood cells. The concentration time curves for evacetrapib and total radioactivity are shown in Figure 1.

Excretion and mass balance

The total recovery of radioactivity in urine and feces samples was 95.4% ($\pm$2.21%) of the dose over the 216-h study collection period, with 85% being recovered in the first 120 h. A mean ($\pm$SD) of 93.1% ($\pm$2.46%) of the dose was excreted in feces and 2.30% ($\pm$0.566%) was excreted in urine. Levels of radioactivity in expired air samples were negligible.

Metabolic profiling

Figure 2 depicts the proposed metabolic scheme of evacetrapib in humans. In plasma, the parent drug evacetrapib, and two metabolites (m): parent + O + 2H (M2), and parent + glucuronide (M10) were detected by radioactivity. Metabolite M2 was the product of oxidative ring opening of the benzazepine to an alcohol. Metabolite M10 was consistent with the standard for the synthetic acyl glucuronide of parent by HPLC retention times and LC/MS/MS spectra (Eli Lilly and Company, unpubl. data). Parent drug was the predominant radioactive peak, accounting for a mean of 94% to 100% of the total radioactivity in the 1- to 8-h plasma samples. In the 24-h plasma samples, parent was the only quantifiable radioactive peak and was detected in only 3 subjects, with evacetrapib concentrations being below the limit of detection in the other 2 subjects. Metabolite M2 accounted for 1% to 4% of the total radioactivity in the 1- to 4-h plasma samples and was below the quantitation limit at 8 and 24 h postdose. Metabolite M10 was quantifiable only in the 2- and 4-h plasma samples, accounting for 1% and 2% of the total radioactivity in the 2- and 4-h plasma samples. Representative radiochromatograms of evacetrapib and metabolites in plasma are shown in Figure 3. In feces, parent drug and 10 metabolites were identified (Table 3). Parent drug, M1, and M7 were the major radioactive peaks in feces, accounting for a mean of 16.80%, 12.24%, and 33.52% of the dose, respectively. Eight minor fecal metabolites were identified including M2, M3 (parent + O), M4 (parent + O), M5 (parent + 2O), M6 (parent + 2O + 2H), M8 (parent + 3O + 2H), M9 (parent + 3O), and M20 (parent + 3O − C8H12O2, *N*-desmethyl cyclohexyl carboxylic acid). Each of these 8 metabolites accounted for less than 5% of the dose. Approximately 70% of the administered evacetrapib dose was eliminated via CYP-mediated metabolism.

Table 1. Predictions of evacetrapib CL_{int} and f_m by CYPs in the in vitro study.

rCYP	$-k_{dep}$ (min^{-1})	CL_{int} (μL $\times$ min^{-1} $\times$ pmol CYP^{-1})	RAF (pmol CYP $\times$ mg^{-1})	HLM Scaled CL_{int}, (μL $\times$ min^{-1} $\times$ mg^{-1})	f_mCYP	Predicted AUC ratio (AUCi/AUC)
CYP2C8	0.0424	0.712	28.0	19.9	0.1	1.1
CYP3A[1]	0.1565	4.257	43.7	186.0	0.9	2.7

$-k_{dep}$, the negative of the depletion rate constant; CL_{int}, intrinsic clearance; f_mCYP, fraction of hepatic CYP-mediated clearance; HLM, human liver microsomes; RAF, relative activity factor; rCYP, human recombinant CYPs.

[1]For determinations of f_m, CYP3A4-mediated metabolism was considered to represent total CPY3A-mediated metabolism AUCi/AUC = 1/(1-f_mCYP3A $\times$ fraction of evacetrapib eliminated by CYPs) where the fraction of evacetrapib eliminated by CYPs is approximately 0.7.

Table 2. Geometric mean (coefficient of variation) pharmacokinetic parameter estimates of evacetrapib and total radioactivity following a single 100-mg oral dose of evacetrapib (containing 100 μCi of [^{14}C]-evacetrapib) in healthy subjects.

Parameter (unit)	Plasma evacetrapib ($N = 5$)	Plasma total radioactivity ($N = 5$)	Blood total radioactivity ($N = 5$)	Average (%) of total radioactivity attributed to evacetrapib	Mean blood-to-plasma ratio
$AUC_{(0-\infty)}$ (ng*hr/mL)[1]	8250 (20)	15,900 (20)	7960 (15)[2]	52	0.501
% $AUC_{(tlast-\infty)}$ (%)[3]	1 (0–4)	19 (13–26)	21 (18–24)[2]		
$AUC_{(0-36)}$ (ng*hr/mL)[1]	6250 (25)	9530 (18)	5570 (14)	66	0.585
C_{max} (ng/mL)[4]	777 (17)	943 (17)	546 (16)	82	0.579
t_{max} (h)[5]	3.02 (1.00–4.00)	3.02 (2.03–4.00)	3.02 (2.03–4.00)		
$t_{1/2}$ (h)[3]	32.3 (20.4–53.9)	39.8 (20.3–63.0)	23.4 (19.8–28.2)[2]		
CL/F (L/h)	12.1 (20)	NC	NC		
V_z/F (L)	564 (50)	NC	NC		
Blood to plasma total radioactivity ratio range	0.518–0.618				
Combined hematocrit (%) Day -1	41.8–45.4				
Combined hematocrit (%) Day 10	42.2–44.9				

$AUC_{(0-36)}$, area under the concentration-time curve from time zero up to 36 h postdose; $AUC_{(0-\infty)}$, area under the plasma concentration versus time curve from time zero extrapolated to infinity; $AUC_{(tlast-\infty)}$, area under the concentration-time curve from time zero to the last time point with a measurable concentration; CL/F, apparent clearance; C_{max}, maximum observed drug concentration; N, number of subjects; NC, not calculated; $t_{1/2}$, apparent terminal half-life; t_{max}, time of C_{max}; V_z/F, apparent volume of distribution during the terminal phase.

[1]Radioactivity units are h·ng-equivalents/mL.
[2]$N = 4$.
[3]Geometric mean (range) data.
[4]Radioactivity units are ng-equivalents/mL.
[5]Median (range) data.

NMR analysis confirmed the structures of the oxidative metabolites M1 and M7 (Fig. 2). Metabolite M1 was the result of hydroxylation of the methyl group, *para* to the nitrogen, of the benzazepine ring-opened metabolite, M2. Metabolite M7 was formed following the same pathways with oxidative ring opening of the benzazepine (M2) and subsequent oxidation of the benzyl alcohol of M1 to a benzoic acid.

Adverse events

Overall, 5 treatment-emergent adverse events (TEAEs) were reported by 2 subjects. The most common TEAEs were diarrhea (2 AEs reported by 1 subject) and headache

(2 AEs reported by 1 subject). Three of the AEs were related to evacetrapib as judged by the investigator. All AEs were of mild severity.

Phase 1 DDI study with ketoconazole in healthy subjects

Pharmacokinetics of evacetrapib

Table 4 summarizes the evacetrapib PK parameter estimates and statistical comparisons with and without ketoconazole. The AUC and C_{max} ratios were 2.37 and 1.94, and the 90% CIs did not include unity. There was no difference in median t_{max} between treatments. Figure 4 illustrates the mean plasma concentration versus time profiles
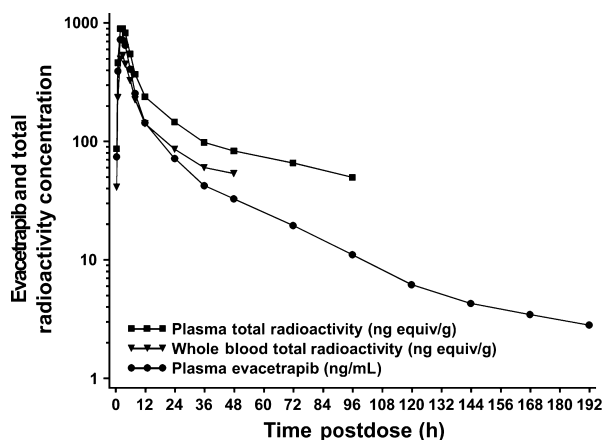
Figure 1. Arithmetic mean (±SD) concentrations of LY2484595 in plasma and total radioactivity in whole blood and plasma after oral administration of a single 100-mg dose of LY2484595 containing approximately 100 μCi of [¹⁴C] LY2484595 in healthy male subjects (semi logarithmic plot).

of evacetrapib following 100 mg evacetrapib alone and with 400 mg ketoconazole.

Adverse events

Of patients receiving evacetrapib alone or in combination with ketoconazole, a total of 18 TEAEs were reported by 5 subjects; 16 TEAEs were considered mild and 2 were considered moderate and all were considered related to the study drug. The two moderate TEAEs were reported by subjects who received ketoconazole alone. The most common TEAEs were headache, nausea, skin disorders, and generalized pruritus.

Phase 1 DDI study with gemfibrozil in healthy subjects

Pharmacokinetics of evacetrapib

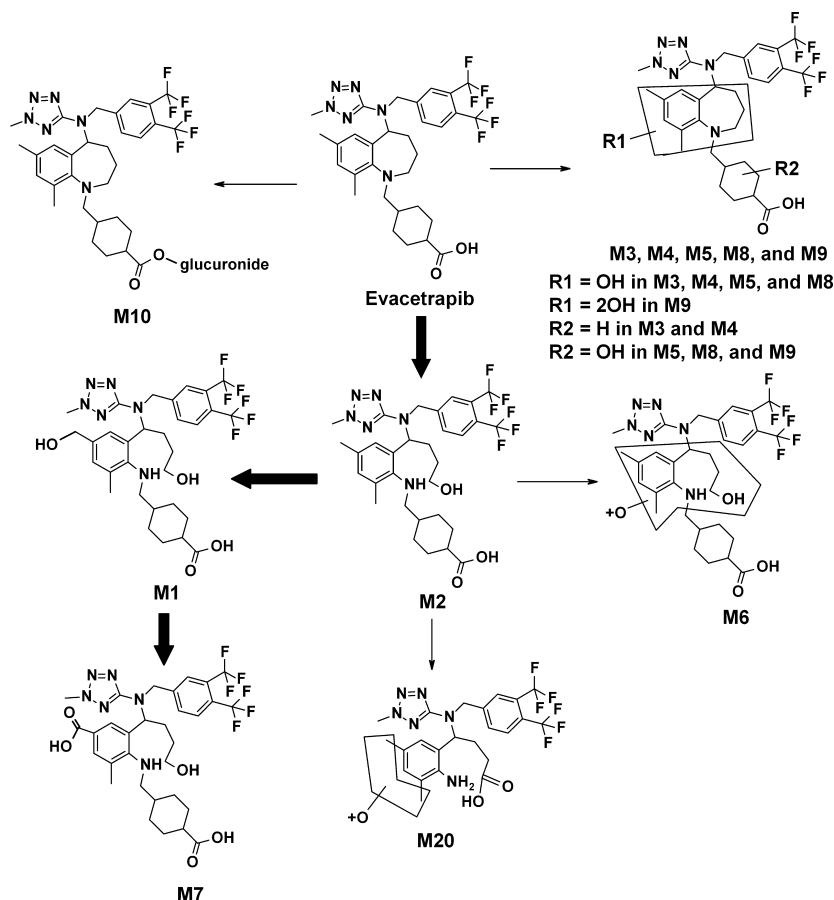Figure 5 illustrates the mean plasma concentration versus time profiles for evacetrapib alone and with gemfibrozil.

Figure 2. Proposed metabolic scheme of evacetrapib in healthy humans following a single oral dose of 100 mg (100 μCi) ¹⁴C-evacetrapib. The heavy bolded arrows represent the major metabolic pathway.

Table 5 summarizes the evacetrapib PK parameter estimates and statistical comparisons with and without gemfibrozil. Data regarding the effects of evacetrapib on gemfibrozil are beyond the scope of this manuscript and, therefore, not shown. Statistical analysis showed no difference in evacetrapib $AUC_{(0-\tau)}$ or C_{max} between treatments, with 90% CIs falling within the no-effect boundary of 0.8–1.25. There was no significant difference in median t_{max}.

Adverse events

During Period 2, three subjects discontinued due to adverse events; 1 subject with an adverse event discontinued during Period 3. A total of 28 AEs were reported by a total of 12 subjects. All of the AEs were mild in severity. Of the 24 subjects who received one or more doses of evacetrapib alone and/or with gemfibrozil, 5 subjects reported a total of 10 AEs considered to be related to the study drug. The most common AE related to the study drug was pruritus (2 AEs reported by 2 subjects). The overall AE profile was similar following evacetrapib administered alone and with gemfibrozil. There was no difference in the frequency of related AEs between these two treatments.

Discussion

Data from the in vitro studies suggest that the oxidative metabolism of evacetrapib predominantly by CYP3A, with a minor contribution by CYP2C8. The clinical disposition study confirmed that evacetrapib is extensively metabolized, and that the principal route of excretion of parent and metabolites is via the feces.

Circulating metabolites of evacetrapib were present, as indicated by levels of total radioactivity that were greater than represented by intact evacetrapib. Two major (>10% of dose) metabolites of evacetrapib were identified in the feces accounting for about half of the administered dose. Including multiple minor metabolites, oxidative metabolism accounted for approximately 70% of the dose, of which about half can be attributed to the major metabolic pathway (M2 → M1 → M7) in feces. The M2 metabolite is formed as the result of the oxidation of the carbon alpha to the nitrogen of the benzazepine ring, with subsequent ring-opening and reduction to yield the corresponding alcohol. Subsequent oxidation of the methyl group (para to the nitrogen) of the di-methyl benzazepine ring also forms an alcohol resulting in formation of the penultimate, M1 metabolite. Metabolite M1 undergoes an additional oxidation reaction resulting in formation of a benzoic acid moiety, resulting in M7. The direct acyl glucuronide metabolite was not detected in feces, but it is
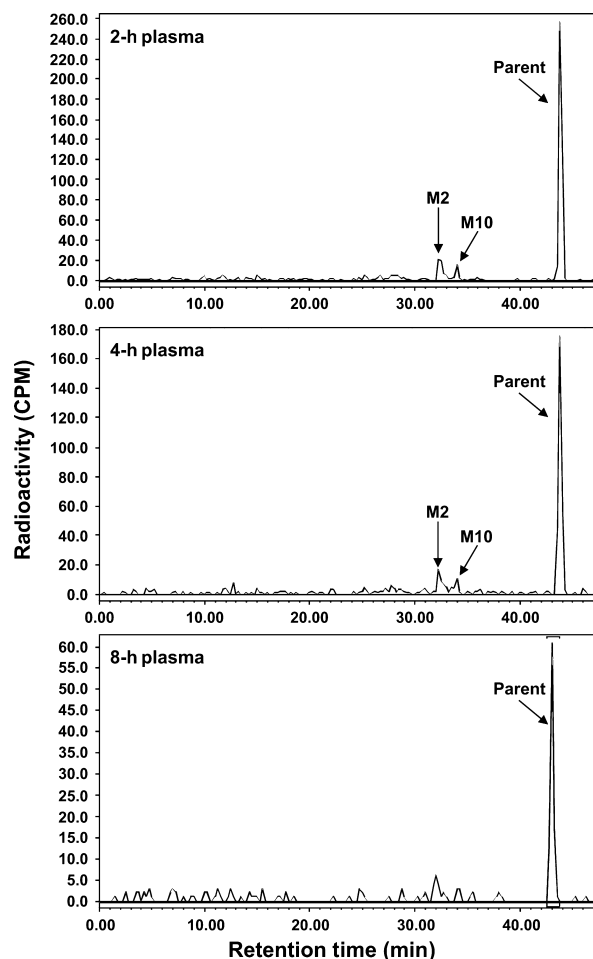

Figure 3. HPLC radiochromatograms of plasma from a healthy human subject after a single oral dose of 100 mg (100 μCi) ^{14}C-evacetrapib. M2 is benzazepine ring-opened metabolite and M10 is the acyl glucuronide metabolite. CPM, counts per minute.

possible that some of the parent drug observed in feces (17%) is a result of hydrolysis/cleavage of the glucuronide metabolite back to intact parent.

The major metabolic pathway for evacetrapib (M2 → M1 → M7) accounts for approximately half of evacetrapib's elimination. Per the FDA and EMA guidances for drug interaction studies, if elimination through a particular pathway is >25%, conducting a study with strong inhibitor (e.g., ketoconazole) is recommended (U.S. Department of Health and Human Services, Food and Drug Administration (FDA) Center for Drug Evaluation and Research (CDER) 2012). In this case, the static model-based predicted ratio of AUC with/without ketoconazole was 2.7, whereas the experimentally determined ratio was 2.37, indicating a good correlation between the predicted effect and the actual clinical results. When evacetrapib was administered with gemfibrozil, a strong

Table 3. Mean percent dose of evacetrapib and its metabolites excreted in feces following a single oral dose of 100 mg (100 μCi) ^{14}C-evacetrapib.

Peak	Percent dose mean	SD
M7	33.52	7.25
M8	2.19	0.61
M9	3.79	1.27
M20	3.41	0.62
M1	12.24	2.33
M6	0.78	0.44
M5	4.62	0.82
M3	1.80	1.30
M2	4.65	0.81
M4	2.20	1.57
Evacetrapib	16.80	6.73
Total % identified	85.99	2.88
Total % metabolites identified	69.2	
Dose eliminated in the select feces through 192 h postdose	89.86	1.82

Figure 4. Semi-log plot of mean plasma evacetrapib concentrations versus time following a 100 mg dose of evacetrapib alone or with 400 mg of ketoconazole (Cannady et al. 2013).

Figure 5. Semi-log plot of mean plasma evacetrapib concentrations versus time following 130 mg evacetrapib QD alone or with 600 mg gemfibrozil BID in healthy subjects. BID, twice daily; QD, daily.

CYP2C8 inhibitor, evacetrapib exposure at steady state was not affected, which is also consistent with the static model prediction for inhibition of CYP2C8. This suggests that CYP2C8 does not play a clinically important role in the clearance of evacetrapib, despite its identification as a contributing metabolic enzyme in vitro. Moreover, the greater degree of variability between the mean concentration versus time profiles of evacetrapib with/without ketoconazole compared with those with/without gemfibrozil is consistent with the reported PK variability of orally administered CYP3A substrates before and after inhibition (Frechen et al. 2013).

Table 4. Summary of evacetrapib noncompartmental pharmacokinetic parameter estimates following 100 mg evacetrapib alone or with 400 mg ketoconazole in healthy subjects.
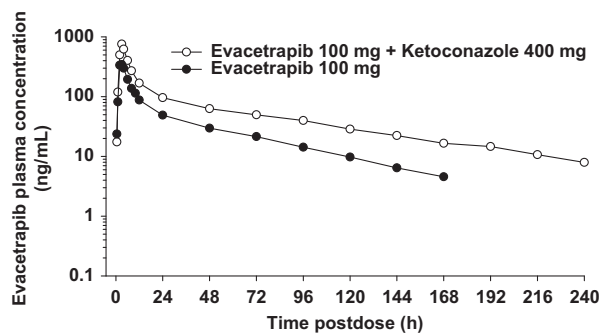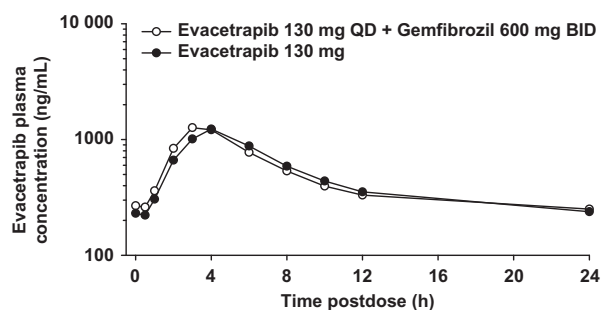
Parameter[3]	Geometric mean (% CV)		Ratio of geometric LS means evacetrapib + ketoconazole versus evacetrapib (90% CI)
	Evacetrapib	Evacetrapib + ketoconazole	
N	12	9	9/12
AUC$_{(0-\infty)}$ (ng·h/mL)	5260 (51)	12,100 (57)	2.37 (1.77, 3.18)
C_{max} (ng/mL)	332 (79)	611 (73)[3]	1.94 (1.39, 2.72)
t_{max}[1] (h)	3.00 (2.00–4.00)	3.00 (2.00–3.00)[3]	–
$t_{1/2}$[2] (h)	40.2 (28.4–55.4)	63.2 (52.1–82.3)	–
CL/F (L/h)	19.0 (51)	8.24 (57)	–
V_{ss}/F (L)	861 (60)	592 (70)	–

AUC$_{(0-\infty)}$, area under the plasma concentration versus time curve from time zero extrapolated to infinity; CI, confidence interval; CL/F, apparent clearance; C_{max}, maximum observed drug concentration; CV, coefficient of variation; N, number of subjects; $t_{1/2}$, apparent terminal half-life; t_{max}, time of C_{max}; V_{ss}/F, apparent volume of distribution at steady state.
[1]Median (range).
[2]Geometric mean (range).
[3]N = 10.

Table 5. Summary of evacetrapib pharmacokinetic parameter estimates following 130 mg evacetrapib QD alone or with 600 mg gemfibrozil BID in healthy subjects.

Parameter	Geometric mean (% CV)		Ratio of geometric LS means evacetrapib + gemfibrozil versus evacetrapib (90% CI)
	Evacetrapib (Day 11)	Evacetrapib + gemfibrozil (Day 22)	
N	22	20	22/20
$AUC_{(0-\tau)}$ (ng·h/mL)	11,300 (20)	11,400 (21)[2]	0.996 (0.922, 1.08)
C_{max} (ng/mL)	1270 (26)	1290 (26)	1.02 (0.933, 1.11)
t_{max}[1] (h)	4.00 (2.02–6.00)	3.00 (2.00–4.00)	—[3]

$AUC_{(0-\tau)}$ = area under the concentration-time curve during one dosing interval; C_{max} = maximum observed drug concentration; CV = coefficient of variation; N = number of subjects; t_{max} = time of maximum observed drug concentration.
[1]Median (range).
[2]N = 19.
[3]Parameters dependent on the terminal phase, such as half-life, were not calculated because the sampling interval was limited to 24 h postdose and did not include the terminal phase.

Historically, ketoconazole (400 mg for ≥5 days) has been considered the "gold standard" strong CYP3A4 inhibitor for assessing DDIs (Ke et al. 2014) but it is not necessarily specific for this enzyme (Sandström et al. 1999). In addition to inhibiting CYP3A, ketoconazole is also a known P-glycoprotein (P-gp) inhibitor; however, Sandström et al. (1999) report that ketoconazole is a more potent inhibitor of CYP3A than P-gp. While the selection of ketoconazole as a probe inhibitor does not allow differentiation of enzyme versus transporter effects, the study design did allow assessment of a worst-case scenario evaluating evacetrapib as a dual CYP3A and P-gp substrate, in the absence of in vitro P-gp data.

Since ketoconazole approximately doubled the exposure of evacetrapib, evacetrapib would not be classified as a sensitive CYP3A substrate as defined by the FDA and EMA guidances, where a sensitive substrate demonstrates ≥5-fold change in exposure (U.S. Department of Health and Human Services, Food and Drug Administration (FDA) CDER 2012; European Medicines Agency 2012). In our study, ketoconazole was effectively a moderate inhibitor of the apparent clearance of evacetrapib. Although exposures of evacetrapib increased in the presence of ketoconazole, the magnitude of the effect was only modest and not clinically meaningful based upon the currently known safety profile of evacetrapib, which includes patients with similar exposures (Eli Lilly and Company, unpubl. data). While this outcome was initially surprising, given the substantial CYP3A-mediated elimination of drug and metabolites via feces, it was consistent with the observation that only minor metabolites appear in circulation (Fig. 3). In addition, the modest effect of ketoconazole on evacetrapib exposure and absence of effect of gemfibrozil on evacetrapib exposure may be a result of numerous interdependent factors, including poor drug solubility, high protein binding, and involvement of alternative clearance pathways such as direct glucuronidation and/or biliary excretion of unchanged drug (Mantlo and Escribano 2014; Cannady 2013). In phase 1 studies, evacetrapib was generally well-tolerated in healthy subjects when administered alone and with ketoconazole or gemfibrozil. The overall severity of AE profile was similar among studies following evacetrapib alone and with ketoconazole or gemfibrozil. Because a very strong CYP3A inhibitor only caused a modest change in evacetrapib exposure and did not increase adverse events (Suico 2014), less potent inhibitors would be expected to have lesser impact on exposure and/or safety. While PBPK modeling is an approach that could be used to predict evacetrapib exposures in the presence of these less potent moderate and weak inhibitors, it appears unnecessary to evaluate their effects on evacetrapib clearance in actual clinical studies.

In conclusion, although the potential exists for evacetrapib exposure to be modestly increased by a strong CYP3A inhibitor, there is a low likelihood of clinically relevant DDIs with co-administered inhibitors at the phase 3 dose of evacetrapib (130 mg) due to the currently known disposition and safety profile of evacetrapib. Taken together, the results described above and collected from ongoing phase 3 studies will provide physicians with information needed to evaluate the appropriateness of evacetrapib when co-administered with any strong CYP3A inhibitor.

Acknowledgements

References

Barter PJ, Brewer Jr HB, Chapman MJ, Hennekens CH, Rader DJ, Tall AR (2003). Colesteryl ester transfer protein: a novel target for raising HDL and inhibiting atherosclerosis. Atheroscler Thromb Vasc Biol 23: 160–167.

Brown BG, Zhao XQ, Chait A, Fisher LD, Cheung MC, Morse JS, et al. (2001). Simvastatin and niacin antioxidant vitamins, or the combination for the prevention of coronary disease. N Engl J Med 345: 1583–1592.

Cannady EA, Rehmel JF, Freidrich S, Zhang W, Krueger KA, Suico JG (2013). The involvement of CYP3A in the clearance of evacetrapib and the effect of co-administration of ketoconazole on the pharmacokinetics of evacetrapib in healthy subjects. American Society for Clinical Pharmacology and Therapeutics (ASCPT); 5–9 March 2013. Poster #PI-30.

Cannon CP, Braunwald E, McCabe CH, Rader DJ, Rouleau JL, Belder R, et al. (2004). Intensive versus moderate and lipid lowering with statins after acute coronary syndromes. N Engl J Med 350: 1495–1504.

European Medicines Agency. 2012. Guidelines on the investigation of drug interactions. Available at http://www.ema.europa.eu/docs/en_GB/document_library/Scientific_guideline/2012/07/WC500129606.pdf (accessed 11 February 2015).

Fahmi OA, Maurer TS, Kish M, Cardenas E, Boldt S, Nettleton D (2008). A combined model for predicting CYP3A4 clinical net drug-drug interaction based on CYP3A4 inhibition,

inactivation, and induction determined in vitro. Drug Metab Dispos 36: 1698–1708.

Frechen S, Junge L, Saari TI, Suleiman AA, Rokitta D, Neuvonen PJ, et al. (2013). A semiphysiological population pharmacokinetic model for dynamic inhibition of liver and gut wall cytochrome P450 3A by voriconazole. Clin Pharmacokinet 52: 763–781.

deGoma EM, Leeper NJ, Heidenreich PA (2008). Clinical significance of high-density lipoprotein cholesterol in patients with low low-density lipoprotein cholesterol. J Am Coll Cardiol 51: 49–55.

Han B, Mao J, Chien JY, Hall SD (2013). Optimization of drug-drug interaction study design: comparison of minimal physiologically-based pharmacokinetic models on prediction of CYP3A inhibition by ketoconazole. Drug Metab Dispos 41: 1329–1338.

Heart Protection Study Collaborative Group. (2002). MRC/BHF Heart Protection Study of cholesterol lowering with simvastatin in 20,536 high-risk individuals: a randomised placebo-controlled trial. Lancet 360: 7–22.

Honkalammi J, Niemi M, Neuvonen PJ, Backman JT (2012). Gemfibrozil is a strong inactivator of CYP2C8 in very small multiple doses. Clin Pharmacol Ther 91(5): 846–855.

Joy TR, Hegele RA (2008). The failure of torcetrapib: what have we learned? Br J Pharmacol 154: 1379–1381.

Ke AB, Zamek-Gliszczynski MJ, Higgins JW, Hall SD (2014). Itraconazole and clarithromycin as ketoconazole alternatives for clinical CYP3A inhibition studies. Clin Pharma Ther 95: 473–476.

Mantlo NB, Escribano A (2014). Update on the discovery and development of cholesteryl ester transfer protein inhibitors for reducing residual cardiovascular risk. J Med Chem 57: 1–17.

Nicholls SJ, Brewer HB, Kastelein JJ, Krueger KA, Wang M-D, Shao M, et al. (2011). Effects of CETP inhibitor evacetrapib administered as monotherapy or in combination with statins on HDL and LDL cholesterol: a randomized controlled trial. JAMA 306: 2099–2109.

Robins SJ, Collins D, Wittes JT, Papademetriou V, Deedwania PC, Schaefer EJ, et al. (2001). Veterans affairs high-density lipoprotein intervention trial. Relation of gemfibrozil treatment and lipid levels with major coronary events. VA-HIT: a randomized controlled trial. JAMA 285: 1585–1591.

Sandström R, Knutson TW, Knutson L, Jansson B, Lennernäs H (1999). The effect of ketoconazole on the jejunal permeability of CYP3A metabolism of (R/S)-verapamil in humans. Br J Clin Pharmacol 48: 180–189.

Sever PS, Dahlof B, Poulter NR, Wedel H, Beevers G, Caulfield M, et al. (2003). Prevention of coronary and stroke events with atorvastatin in hypertensive patients who have average or lower-than-average cholesterol concentrations, in the

Anglo-Scandanavian Cardiac Outcomes Trial-Lipid Lowering Arm (ASCOT-LLA): a multicentre randomised controlled trial. Lancet 361: 1149–1158.

Shepherd J, Blauw GJ, Murphy MB, Bollen ELEM, Buckley BM, Cobbe SM, et al. (2002). Pravastatin in elderly individuals at risk of vascular disease (PROSPER): a randomised controlled trial. PROspective Study of Pravastatin in the Elderly at Risk. Lancet 360: 1623–1630.

Suico JG, Friedrich S, Krueger KA, Zhang W (2014). Evacetrapib at a supratherapeutic steady state concentration does not prolong QT in a thorough QT/QTc study in healthy participant. J Cardiovasc Pharmacol Ther 19: 283–289.

U.S. Department of Health and Human Services, Food and Drug Administration (FDA) Center for Drug Evaluation and Research (CDER). (2012). Guidance for industry: study design, data analysis, implications for dosing, and labeling recommendations. Available at http://www.fda.gov/downloads/drugs/guidancecomplianceregulatoryinformation/guidances/ucm292362.pdf (accessed 02 December 2014).

Wickremsinhe ER, Hynes SM, Palmieri MD, Mitchell MI, Abraham TL, Fayer Rehmel J, et al. (2014). Disposition and metabolism of LY2603618, a Chk-1 inhibitor following intravenouse administration in patients with advanced and/or metastatic solid tumors. Xenobiotica 44: 827–841.

Zhao P, Pagueneau-Majlessi I, Zhang L, Strong JM, Reynolds KS, Levy RH, et al. (2009). Quantitative evaluation of pharmacokinetic inhibition of CYP3A substrates by ketoconazole: a simulation study. J Clin Pharmacol 49: 351–359.

Supporting Information

Additional Supporting Information may be found in the online version of this article:

Figure S1. Phase 1 drug–drug interaction study with ketoconazole in healthy subjects.
Figure S2. Phase 1 drug–drug interaction study with gemfibrozil in healthy subjects.